Title Page

Maternal-Fetal Disposition and Metabolism of Retrorsine in Pregnant Rats

Xia Li, Xiaojing Yang, E Xiang, Jinyuan Luo, Shuaikai Qiu, Yan Fang, Li Zhang, Yu Guo, Jiang Zheng, Hui Wang

Department of Pharmacology, School of Basic Medical Science, Wuhan University, Wuhan 430071, P. R. China (X. L., E. X., J. L., S. Q., Y. F., Y. G., H. W.); Hubei Provincial Key Laboratory of Developmentally Originated Disease, Wuhan 430071, P. R. China (X. L., E. X., J. L., S. Q., Y. F., Y. G., H. W.); Wuya College of Innovation, Shenyang Pharmaceutical University, Shenyang, Liaoning, 110016, P. R. China (X. Y., J. Z.); State Key Laboratory of Functions and Applications of Medicinal Plants (J. Z.), Key Laboratory of Pharmaceutics of Guizhou Province, Guizhou Medical University, Guiyang, Guizhou, 550004, P. R. China (J. Z.)

Running Title Page

Running title: Intrauterine Disposition and Metabolism of Retrorsine in Rats

Corresponding Authors:

Yu Guo

Department of Pharmacology, School of Basic Medical Science, Wuhan University, Wuhan 430071, P. R. China; Hubei Provincial Key Laboratory of Developmentally Originated Disease, Wuhan 430071, P. R. China

E-mail: guoy@whu.edu.cn
Tel: +86-27-68758665
Fax: +86-27-68759222

Jiang Zheng

[1]Wuya College of Innovation, Shenyang Pharmaceutical University, Shenyang, Liaoning, 110016, P. R. China; [2]State Key Laboratory of Functions and Applications of Medicinal Plants, Key Laboratory of Pharmaceutics of Guizhou Province, Guizhou Medical University, Guiyang, Guizhou, 550004, P. R. China

E-mail: zhengneu@yahoo.com
Tel: +86-24-23986361
Fax: +86-24-23986510

The number of text pages: 21
The number of figures: 7
The number of references: 44
The number of words in the *Abstract*: 276
The number of words in the *Introduction*: 625
The number of words in the *Discussion:*: 1231

Abbreviations

pyrrolizidine alkaloids, PAs; cytochrome P450, CYP; retrorsine, RTS; gestation day, GD; glutathione, GSH; glyceraldehyde phosphate dehydrogenase, GAPDH; 4-dimethylaminobenzaldehyde, DABA; hematoxylin and eosin, HE; declustering potential, DP; collision energy, CE; collision cell exit potential, CXP; high-performance liquid chromatography, HPLC; multiple-reaction monitoring, MRM; ATP-binding cassette, ABC

Abstract

Pyrrolizidine alkaloids (PAs) are extensively synthesized by plants and are commonly present in herbs and foodstuffs, which exhibit hepatotoxicity requiring metabolic activation by cytochrome P450 (CYP) 3A to form the electrophilic metabolites－pyrrolic esters. PAs also cause embryo toxicity, but the metabolic profiles of PAs in fetus and placenta have been far from clear. In this study, we determined the basal metabolic activation of retrorsine (RTS) in rat maternal liver, placenta and fetal liver *in vitro*, and examined the fetal toxicity and bioactivation of RTS *in vivo*. Detection of microsomal RTS metabolites *in vitro* showed that the basal metabolic activity of fetal liver and placenta to RTS was much weaker than that of maternal liver. In addition, higher rate of pyrrolic ester formation was found in normal male fetal liver, compared with that of female pups. *In vivo* exposure to RTS caused fetal growth retardation as well as placenta and fetal liver injury. Little difference in serum RTS was observed in dams and fetuses, but the content of pyrrole-protein adduction in fetal liver was much lower than that in mother liver, which was consistent with basal metabolic activity. Unexpectedly, compared with basal metabolism in fetal liver, exposure to RTS during middle and late pregnancy caused an opposite gender difference in RTS metabolism and CYP3A expression in fetal liver. For the first time, our study proved that RTS was capable of permeating placenta barrier and entering fetal circulation, while the intrauterine pyrrolic metabolite was mainly generated by fetal liver, but not transported from mother circulation. Induction of CYP3A by RTS was gender-dependent in fetal liver, which was probably responsible for RTS-induced fetal

hepatic injury, especially for female pups.

Introduction

Pyrrolizidine alkaloids (PAs) are a type of defense constituents with similar chemical structure and wildly present in plants. PAs have been attracting attention due to their severe hepatotoxicity and wide range of sources placing humans at a high risk for exposure. Approximately 3% of flowering plants contain toxic PAs, and 660 kinds of PAs and their *N*-oxide metabolites have been found in more than 6000 plants in worldwide (Radominska-Pandya 2010; Smith and Culvenor, 1981). Many foodstuffs, such as milk, honey, eggs, tea and plant spices were reportedly contaminated by PAs (Huybrechts and Callebaut, 2015). Research showed that unsaturated PAs exhibited notable toxicity after metabolic activation mainly by cytochrome P450 (CYP) 3A to form electrophilic intermediates (pyrrolic esters), which attack a variety of important intracellular nucleophilic substances (e.g. DNA and protein) (Ruan et al. 2015; Yang et al. 2001). Pyrrolic esters can be detoxified by conjugating with glutathione (GSH), and excessive PA exposure may cause depletion of GSH and adduction of DNA and protein, lead to hepatocyte apoptosis and death, and result in hemorrhagic necrosis, liver macrocytosis and vein occlusion (Zhou et al. 2007).

Besides hepatic damage, PAs can also cause embryo toxicity. Hepatic sinusoidal obstruction syndrome was observed in a newborn infant from a mother who drank herbal tea during gestation, and the tea was found to contain detectable level of PA seconine (Roulet et al. 1988). Animal studies reported fetal deaths, weight loss, and teratogenesis in pregnant rats receiving PAs from early pregnancy (Bhattacharyya 1965; Panter et al. 1998; Medeiros et al. 2000). Our early work demonstrated that prenatal exposure to PAs alone or with lipopolysaccharide led to fetal mortality and preterm in

5

mice (Guo et al. 2013).   But many aspects of PA-induced embryo toxicity still remain unclear.   For instance, PAs are presumed to enter fetal blood circulation through placental barrier and associate with embryo toxicity, however, no experimental evidence is available up to date (Sundareson 1942).

In addition, although early research showed that human placenta expressed CYPs 2C, 2D6 and 3A7 during pregnancy (Hakkola et al. 1996a), and rat placenta also contained a variety of CYP isoforms, such as CYP3A1 (Ejiri et al. 2003), whether CYP3A protein in placenta has function to catalyze xenobiotics metabolism is controversial (Hakkola et al. 1996; Maezawa et al. 2010; Fabian et al. 2016).   Most importantly, whether fetal liver has the ability to metabolize PAs needs to be verified, so that we can evaluate the contribution of fetal metabolism to PA-induced embryotoxicity.   Although it has been reported that hepatic CYP3A protein was detectable in both human and rat fetuses (Wyde et al. 2005; Hines, 2008), there was still lack of evidence that toxic metabolites of PAs can be produced by fetal liver.

Furthermore, hepatotoxicity of PAs was reported to show gender difference.   Lin and coworkers found that metabolic activation of clivorine, a naturally occurring pyrrolizidine alkaloid, took place more in adult male rats than in female (Lin et al. 2002, 2003, 2007), which indicates that male rats may be more susceptible to PA-induced toxicity.   In fetus, androgens secreted by developing testis may induce gender-specific patterns of metabolic enzyme activity in liver (O'Shaughnessy 2011).   As such, we assumed that PA metabolism in fetal liver might also exhibit a gender difference.

Retrorsine (RTS, Scheme 1) is a commonly existing and extensively studied PA. Like most PAs, it is also activated by CYP3As in rats (Wang et al., 2005).   The

objectives of the present study were to determine the toxicity and metabolic activation

of RTS in maternal-placental-fetal unit of rats and to examine the gender difference in

RTS metabolism of rat fetuses.   This study intended to seek solid evidence for

metabolic toxicity of RTS in rat placenta and fetus, and may allow us to better

understand the embryotoxicity caused by RTS.

Materials and Methods

1. Reagents

Retrorsine (RTS, ≥98%), monocrotaline (≥98%), diazepam (≥98%), glutathione (GSH, ≥98%), 4-dimethylaminobenzaldehyde (DABA), *S*-hexylglutathione (≥97%), silver nitrate, and NADPH were purchased from Sigma Chemical Co. (St. Louis, MO). Formic acid, trifluoroacetic acid, and perchloric acid were acquired from Fisher Scientific (Springfield, NJ). Goat-anti CYP3A polyclonal antibody was obtained from Santa Cruz (Cat. sc-30621, Dallas, TX). Mouse anti-glyceraldehyde phosphate dehydrogenase (GAPDH) antibody was purchased from Abclonal (Cat. AC002, Wuhan, Hubei, China). All organic solvents were obtained from Fisher Scientific (Springfield, NJ). Other reagents and solvents were either analytical or HPLC grade.

2. Chemical Synthesis

Glutathione conjugates **3-5** (Scheme 1) were synthesized by reaction of dehydromonocrotaline pre-prepared with GSH, following the protocol we published earlier (Chen et al. 2016). Authentic compound **10** was prepared, according to the protocol published in our early paper (Lin et al. 2011; Ruan et al. 2015).

3. Animals and Treatment

Specific pathogen-free (SPF) Wistar rats (female body weight: 200 ± 20 g, male body weight: 280 ± 20 g) were purchased from Experimental Center of Medical Scientific Academy of Hubei Province (China). The animals were allowed free access to food and water at all times, and were maintained on a 12 h light/dark cycle in a

controlled temperature (20 ± 2 °C) room.   All animal experimental procedures were performed in accordance with the Guidelines for the Care and Use of Laboratory Animals of the Chinese Animal Welfare Committee.

Two female rats were mated with one male overnight (from 7:00 pm to 7:00 am next morning).   The day when a vaginal plug was found was designated as gestation day 0 (GD0).   Half of dams without any treatment were sacrificed on GD20, maternal liver, fetal liver and placenta were harvested for microsomes preparation through multistep centrifugation (200 g for 20 min, 9,000 g for 20 min, and 10,500 g for 1 h). The microsomes were stored in -80 °C for further basal metabolism assay and enzyme kinetic study.

The other half of the pregnant rats were intragastrically given vehicle or RTS at various doses from GD9 to GD20.   Animals in control group were treated with vehicle. Rats in groups RTS5, RTS10, and RTS20 were administrated with RTS at 5, 10, or 20 mg/kg, once per day, respectively.   RTS was suspended in water, followed by dropwise addition of dilute HCl solution until the alkaloids were dissolved.   The resulting acidic solution was neutralized by addition of a NaOH solution.   All the dams were euthanized by ether anesthesia or decapitation on GD20, 2 h after retrorsine administration.   Pup body weights were recorded, and simultaneously, maternal and fetal serum and livers as well as placenta were collected for further analysis.

4. Morphological Examination

For retrorsine-treated rats, maternal and fetal livers as well as placenta were fixed with 10% neutral formalin.   Paraffin sections (the thickness was 5 μm) were prepared

and then stained with hematoxylin and eosin (HE). Histomorphological changes of

these tissues were evaluated under light microscopy, and photomicrographs were

captured using Photo Imaging System (Nikon, TE2000). The tissue slides were

obtained from at least three dams per group, and the results were verified independently

by four authors (Xia Li, Jinyuan Luo, Yu Guo and Li Zhang, and Li Zhang is a

pathologist with expertise in morphological examination).

5. Determination of Serum RTS in Dams and Fetuses

Serum levels of RTS were estimated by a reported method with some modification

described by our laboratory (Yang et al. 2017). Aliquots (20 μL) of serum sample

were mixed with 50 μL of acetonitrile containing monocrotaline as the internal standard.

The resulting mixtures were vortex-mixed and centrifuged at 16,000 g for 10 min to

remove the precipitated protein. The resultant supernatants were diluted with three

volumes of water and then subjected to an LC-MS/MS system for analysis.

6. Determination of Pyrrole-protein Adduction in Livers of Maternal and Fetal Rats

Liver tissues (0.2 g) were homogenized in 2 mL of phosphate buffer (pH 7.4, 100

mM), followed by centrifuging at 9,000 g for 10 min. The supernatants were used for

the determination of hepatic protein adduction levels by the method established in our

laboratory (Lin G et al. 2011). Briefly, each liver sample (100 μL) was mixed with

500 μL of acetone, vortexed, and centrifuged at 900 g for 5 min. After being washed

with 500 μL of absolute ethanol, the resulting pellets were reconstituted in 500 μL of

freshly prepared 2% silver nitrate ethanol solution containing 5% trifluoroacetic acid

and were shaken for 30 min at room temperature. After centrifugation at 19,000 g for

10 min, the resulting supernatants were reacted with 4-dimethylaminobenzaldehyde

(v/v 4:1) in ethanol containing 1% perchloric acid at 55 °C for 10 min. To each sample

was added 10 μL of IS (diazepam, 1.25 μg/mL) and the resultant mixtures were injected

into an LC−MS/MS system for analysis. The chemical structure of the molecule

(compound **10**) detected by LC-MS/MS is shown in Scheme 1.

7. Enzyme Kinetic Study

The preparation of rat liver and placenta microsomes were carried out as described

by our laboratory (Lin G et al. 2007). For enzyme kinetic studies, the incubation

mixtures consisted of 0.25 mg/mL microsomal protein (including maternal and fetal rat

liver microsomes and placenta microsomes), 3.2 mM $MgCl_2$, 10 mM GSH, 100 mM

potassium phosphate buffer (pH 7.4), RTS (100-8,000 μM) and 1.0 mM NADPH.

The final volume of each sample was 200 μL, and the total organic concentration of

each incubation mixture was <1% *v/v* acetonitrile. The reaction was stopped by

addition of 200 μL of ice-cold acetonitrile after 20 min incubation at 37 °C. For

comparison, incubations were performed with optimized microsomal protein

concentration and incubation time in their linear ranges. The resulting mixtures were

vortex-mixed and centrifuged at 19,000g for 10 min. The supernatants were diluted

with equal volumes of water and then analyzed by the LC-MS/MS system. All

experiments were performed in triplicate. In the incubation system, the catalytic

capabilities of the enzymes were evaluated by the MS peak areas of pyrrole-GSH

conjugates **4** and **5** (integrated).   GraphPad Prism version 5.04 (GraphPad Software, San Diego, CA) was used in the statistical analyses of enzyme kinetic parameters.

8. LC-MS/MS Method

The quantifications of RTS and its metabolite were performed on an AB SCIEX Instruments 5500 triple quadrupole mass spectrometry (Applied Biosystems, Foster City, CA) equipped with an Agilent 1260 Series Rapid Resolution LC system.   Data were analyzed using Applied Biosystems/SCIEX Analyst software (version 1.6.2). Samples were analyzed by multiple-reaction monitoring (MRM) scanning in positive ion mode.   The optimized MS instrument parameters were as follows: ion spray voltage was set at 5500 V, and ion source temperature was set at 650 °C.   Curtain gas, gas 1, and gas 2 were 20, 50, and 50 psi, respectively.   The characteristics of ion pairs (declustering potential, DP; collision energy, CE; and collision cell exit potential, CXP) and respective LC conditions were listed as follows.

For analysis of RTS, the chromatographic separation was achieved on a Kinetex HILIC (50×2.1 mm, 2.6 μm) column (Phenomenex, Torrance, CA) protected by a Security-Guard (4.0×3.0 mm, 5.0 μm) C18 column (Phenomenex, Torrance, CA). Mobile phase was composed of acetonitrile (A)/ammonium acetate (5 mM, B) with a gradient elution as follows: 0-3.5 min, 15 % B; 3.5-4.5 min, 15-60 % B; 4.5-5.5 min, 60 % B; 5.5-6.5 min, 60-15 % B; 6.5-11 min, 15 % B.   Flow rate was set at 0.4 mL/min. The characteristic ion pair (DP, CE, and CXP) for RTS and monocrotaline (IS) were m/z 352.1→119.9 (100, 48, 10) and m/z 326.1→120.2 (270, 34, 13).

For analysis of pyrrole-protein adduction, the chromatographic separations were

achieved on a CAPCELL PAK UG-C18 column (250×4.6 mm, 5.0 μm) (Shiseido,

Tokyo, Japan) protected by a Security-Guard (4.0×3.0 mm, 5.0 μm) C18 column

(Phenomenex, Torrance, CA).   Mobile phase systems containing acetonitrile with 0.1 %

formic acid (A) and water with 0.1 % formic acid (B) were used with a gradient elution

as follows: 0-2 min, 70-70 % B; 2-10 min, 70-10 % B; 10-12 min, 10-10 % B; 12-14

min, 10-70 % B; and 14-17 min, 70-70 % B.   Flow rate was set at 0.8 mL/min.   The

characteristic ion pairs (DP, CE, and CXP) were m/z 341.0→252.1 (100, 40, 10) for

pyrrole-protein adduction and m/z 285.1→193.5 (101, 46, 10) for diazepam (IS),

respectively.   For determination of pyrrole-GSH conjugates, the chromatographic

separations were also performed on the CAPCELL PAK UG-C18 column system.

Mobile phase system including acetonitrile with 0.1 % formic acid (A) and water with

0.1 % formic acid (B) was used with a gradient elution as follows: 0−2 min, 90−90 %

B; 2−10 min, 90−10 % B; 10−12 min, 10−10 % B; 12−14 min, 10−90 % B; and 14−17

min, 90−90 % B.   Flow rate was 0.8 mL/min.   The parameters of ion pairs (DP, CE,

and CXP) were m/z 425.0→118.0 (100, 30, 13) for GSH conjugate and m/z

392.2→246.3 (86, 24, 5) for S-hexylglutathione (IS), respectively.

9. Western Blot

Protein extraction from retrorsine-treated fetal liver was carried out as described

in protocol of kit (Beyotime Biotechnology, Nantong, Jiangsu, China), and maternal

liver microsomes were used as the positive control.   Protein extracts were separated

in 5%‐10% SDS-PAGE and electrophoretically transferred onto polyvinylidene

fluoride membranes.   After blocking with 5% nonfat milk in phosphate buffer,

13

CYP3A proteins were determined by immunoblot using goat anti-CYP3A antibody, and GAPDH proteins were determined as housekeeping proteins employing mouse anti-GAPDH antibody. Membranes were then incubated with secondary antibodies conjugated with horseradish peroxidase, and specific protein bands were visualized by chemiluminescence detection, according to the manufacturer's protocol (Bridgen, Beijing, China).

10. Statistical Analysis

The data were analyzed using Statistical Package for the Social Sciences version 17.0 software (SPSS Inc, Chicago, IL, USA). Unless stated otherwise, data are presented as mean±SEM. Two-way ANOVA was performed to determine interaction between gender (female and male) and group (control and RTS). Comparison of multiple means with analysis of variance, after the equal check of variance, and individual group means were compared using Bonferroni test. A value of $P<0.05$ was considered significantly different.

Results

1. Basal Metabolism of RTS in Rat Maternal-placental-fetal Unit *in vitro*

RTS was metabolized to a pyrrolic ester via oxidation reaction catalyzed by P450 enzymes, and the reactive metabolite sequentially reacted with GSH to form the corresponding GSH conjugates, and the formation of the GSH conjugates most likely represented the generation of the pyrrolic ester.   As shown in Figure 1, microsomes of normal maternal and fetal livers as well as placenta were able to catalyze the metabolic activation of RTS, but the efficacies varied.   Significantly higher metabolic activation of RTS was observed in maternal liver microsomes than that of the microsomes obtained from fetal liver and placenta ($P<0.01$), while there was no distinct difference in the formation of pyrrole-GSH conjugates in fetal liver and placenta microsomes incubated with RTS.

2. Efficiency to Bioactivate RTS in Maternal and Fetal Liver Microsomes

Michalis-Menten plots and enzyme kinetic parameters are shown in Figure 2 for biotransformation of RTS in normal maternal and fetal livers. K_m and V_{max} values were calculated based on the production of GSH conjugates **4** and **5** (integrated). V_{max} value was greater in maternal liver microsomes than that in fetal liver microsomes, and K_m value of maternal liver microsomes was much less than that of liver microsomes prepared from pups.   Maternal hepatic CL_{int}, calculated by V_{max}/K_m, was 21.9-fold higher than that of female fetal liver microsomes, and was 10.8-fold higher than that of male fetal liver microsomes, respectively.   Besides, male fetal microsomes exhibited a better catalytic activity than female to bioactivate RTS.

15

3. Fetal Toxicity of RTS

As shown in Figure 3, there was no distinct difference in fetal weight between control and low doses of RTS (5 and 10 mg/kg) groups. However, a significant decrease ($P<0.01$) in body weight of pups was observed in dams treated with the high dose (20 mg/kg), compared with that of the control animals. There was no gender difference of fetal body weight in any group.

Little pathohistologic changes in mother liver were detected in the low groups (5.0 and 10 mg/kg) (Figure 4B and C), while swelling and vacuolization of hepatocytes were observed in dams treated with the high dose (20 mg/kg, Figure 4D). Normal rat fetal liver consisted of immature hepatocytes, multinucleated giant cells, and vacuolar parenchyma cells (Figure 4E and I). Increased number of parenchyma cells and loss of hepatocytes were observed in pups of animals given the high dose (Figure 4H and L), especially for female, increased vacuolar cells were seen even in group of dose 10 mg/kg (Figure 4G). Rat placenta comprises decidua (maternal placenta area), junctional and labyrinthine zones (fetal placenta area). Compared with the control group, RTS exposure caused morphology disorder in placenta tissue, especially for the high dose (20 mg/kg, Figure 4N-P and R-T). Necrotic glycogen cells in junctional zones were observed, accompanied with cysts and congestion. Additionally, loss of cells in labyrinthine zone was found, along with irregular arrangement. Placentas of both genders showed similar morphological changes.

4. Levels of RTS in Rat Maternal and Fetal Serum

Elevated serum RTS was observed in both dams and fetuses with the increase of

16

dosing. The level of RTS in fetal sera was proportional to that in maternal sera, and there was no difference in serum RTS between two genders of pups (Figure 5). It suggests that most RTS circulated in maternal blood permeated rat placenta and entered fetal blood flow.

5. Pyrrole-protein Adduction in Maternal-placental-fetal Unit *in vivo*

The levels of hepatic pyrrole-protein adduction in mice given RTS were assessed by chemical derivatization of the protein adducts to compound **10** (Scheme 1). As shown in Figure 6, pyrrole-protein adduction was detected in maternal and fetal liver as well as placenta from dams administered with RTS. The contents of pyrrole-protein adducts formed in placenta of female pups were about 36.7%, 45.2% and 69.9% of maternal hepatic pyrrole protein adduction in groups 5.0, 10 and 20 mg/kg, respectively. The levels of pyrrole-protein adduction in male fetal placenta were similar to that in placenta of female pups. There was no gender difference of placental pyrrole protein adduct content.

RTS-induced protein adduction in fetal liver was much less than that in maternal liver and placenta. Although fetal hepatic pyrrole-protein adduction increased in a dose-dependent manner, the levels of pyrrole-protein adduction in female and male pups exposed to RTS at 20 mg/kg were only 9.0% and 4.8% of maternal hepatic pyrrole-protein adduction, respectively ($P<0.01$). According to two-way ANOVA analysis, there was no interaction between gender and RTS treatment, but there was a significant gender difference of pyrrole-protein adduction content in fetal liver. The levels of pyrrole-protein adduction in female fetal liver were higher than that in male fetal liver ($P<0.01$).

17

6. Effect of RTS Treatment on CYP3A Expression in Fetal Liver

Expression of hepatic CYP3A was higher in male fetuses than that in female pups from dams treated with vehicle ($P<0.01$, Figure 7).   There was an interaction between fetal gender and RTS treatment.   Prenatal RTS exposure significantly induced CYP3A expression in female fetal liver ($P<0.01$), while down-regulated CYP3A protein content was observed in male fetal liver ($P<0.01$).

Discussion

Early study demonstrated that CYP3A enzyme was responsible for metabolic activation of RTS (Wang et al. 2005). To determine the role of fetal hepatic and placental CYP3A in bioactivation of RTS and RTS-induced fetal toxicity, we assessed the basal metabolic activity of CYP3A in fetal liver and placenta obtained from normal pregnant rats on GD 20. It is evident that rat fetal liver and placenta were capable of catalyzing RTS metabolism (Figure 1), though the basal catalytic efficiency of fetal CYP3A was lower than that in maternal liver. In addition, the results showed that basal metabolic efficiency of RTS in male fetal liver were higher than that in female, which is consistent with previous report of gender-difference in CYP3A expression and PA metabolic activation in adult rats (Lin et al. 2002, 2003, 2007).

To better understand the relationship between RTS-induced fetal toxicity and *in situ* RTS metabolic activation in placenta and fetal liver, we established a prenatal-RTS-exposure rat model, and started with the investigation of changes in fetal body weight as well as in hepatic and placental morphology in prenatal RTS-exposed rats. Prenatal exposure to RTS at 20 mg/kg during second and third trimester led to a reduction of rat fetal body weight, which verifies previous reports that PA induced developmental retardation in rats (Medeiros et al. 2000; Sandini et al. 2014; Peterson and Jago, 1982). Remarkable paramorphia of placental trophoblast and fetal hepatocytes were observed in animals treated with RTS at 20 mg/kg (Figure 4). Developing liver appeared to be more susceptible to this reactive hepatotoxicant, manifested by significant pathological changes of fetal liver but slightly swelling of

19

maternal hepatocyte (Figure 4). Then we examined the parent RTS and pyrrole-protein adduction in utero. It has been speculated that PA was able to permeate placenta (Sundareson 1942), but no experimental evidence was available in support of the speculation until our study. The level of RTS in fetal sera was similar as that in mother sera, especially for high dose group (Figure 5). Barrier role of ATP-binding cassette (ABC) transporters, especially P-glycoprotein, in placenta was stressed by Lankas and his colleagues (Lankas et al. 1998), but Tu et al. reported that RTS is a weak substrate for P-glycoprotein (Tu et al. 2014). We guess that may be the reason why RTS entered rat fetus through placenta barrier almost without obstacle.

Pyrrolic esters are the main toxic metabolites of PAs. Because of their electrophilic reactivity, pyrrolic esters attack nucleophilic sites of protein to form pyrrole protein adduction after generated from parent PAs *in situ*, and the protein modification may trigger the hepatotoxicity of PAs. A considerable amount of pyrrole protein adducts was observed in placenta in rats prenatally exposed to RTS. Although we confirmed metabolic activation of RTS in placenta *in vitro*, we cannot exclude the possibility that the reactive metabolite of RTS generated in maternal liver can be transported to placenta with blood flow and then exerted their toxicity by reacting with protein in placenta. The reason for this speculation is that pyrrolic ester-derived GSH conjugate in placental microsomes was found to be only 10% of that in maternal liver microsomes *in vitro*, while similar levels of pyrrole-protein adduction were found in placenta and maternal liver *in vivo*. It suggests that the reactive metabolite of RTS formed through maternal bioactivation probably participated, at least in part, in the

placenta metabolic injury.

Pyrrole-protein adduction took place less in fetal liver than those in maternal liver and placenta in animals given RTS (Figure 6). However, minor changes in histopathology were observed in maternal liver tissues. The explanation could be that developing embryo has relatively low levels of CYP3A, which leads to the lower amount of pyrrole-protein adduction observed in fetal liver. Some critical detoxifying enzymes, such as glutathione *S*-transferases, are also much less in fetal than that in mother liver (Wells et al., 2009). And activities of most antioxidative enzymes in embryonic liver are only around 5% of that in maternal liver (Wells et al., 2005). In addition, fetuses are more susceptible to genetic damage than adults. After exposure to tobacco smoke for 20 days, fetuses showed greater DNA damage than the dams (Florek et al., 1999). The above factors may contribute to the high susceptibility of fetus to reactive intermediate-mediated toxicity such as RTS-induced liver injury.

Local metabolic activation seems to be the primary cause of RTS-induced fetal liver toxicity. Juchau and coworkers mentioned that exported reactive intermediates generated from maternal liver were unlikely to reach embryonic targets and were impossible to pass through chorioallantoic and/or yolk sac membranes from maternal systemic circulation (Juchau et al. 1989). The present study clearly demonstrated a weak but certain RTS metabolism in normal fetal liver. The weak basal metabolic activation of RTS by fetal liver microsomes *in vitro* is in agreement with the low level of pyrrole protein adduct generation in pup liver *in vivo*. Since pyrrole protein adduct is a definite marker for PA toxicity (Gao et al. 2015; Ruan et al. 2015; Xia et al. 2016),

our result suggests that the fetal hepatotoxicity may arose from the formation of protein

adduction derived from electrophilic intermediates of RTS, mainly formed *in situ* and

mediated by fetal hepatic CYP3A. Moreover, it is well known that placenta is an

important pregnancy maintenance tissue and responsible for nutrients and oxygen

exchanges between mother and fetus (Longo and Reynolds, 2010). Fetal growth

retardation may happen if the placenta was impaired chronically (İskender-Mazman et

al. 2014). It is likely that PA-induced fetal toxicity in rats partially resulted from

placenta injury.

In normal physiological condition, CYP3A expression in male liver is higher than

female, both for adult (Lin et al. 2002, 2003, 2007) and fetal rats (Figure 7).

Interestingly, our results showed that RTS caused a sexual dimorphic induction of

CYP3A. Apparently, RTS induced hepatic CYP3A expression in female fetus, while

the alkaloid attenuated the expression of the protein in male fetus, which resulted in the

observed gender-related metabolic difference of RTS in fetal rats *in vivo* (Figure 6 and

7). Previous study did not show CYP3A induction by a single dose of 30 mg/kg RTS

in male Fischer 344 rats (Gordon et al. 2000), but our results demonstrated an increase

of CYP3A protein level in fetal liver after a 12-day exposure to RTS, and we found for

the first time that RTS exposure led to a gender-specific induction of CYP3A. Such

gender-specific CYP3A induction by other chemical inducers in adult rats was also

documented, including methoxychlor, dichlorodiphenyltrichloroethane, pregnenolone

16α-carbonitrile, and rifampin (Sierra-Santoyo et al. 2000; Oropeza-Hernández et al.

2003; Gorski et al. 2003; Jan et al. 2006), but the mechanisms of female-specific

22

induction of CYP3A remain unknown.

In summary, the present study examined the metabolic activity of RTS in maternal-placental-fetal unit *in vitro*, and evaluated embryo toxicity and fetal local metabolic activation of the PA *in vivo*. The main conclusions included the following points: 1) rat fetal liver and placenta was capable to metabolize RTS; 2) prenatal exposure to RTS caused remarkable organ/tissue injury and loss of fetal body weight; 3) RTS almost permeated "placenta barrier" completely, but the levels of the resulting pyrrole-protein adduction varied in maternal liver, fetal liver, and placenta; 4) more pyrrole-protein adduction took place in female pups than in male；and 5) the observed female-specific metabolic activation of RTS may arise from higher CYP3A expression in female fetal liver, induced by long-term exposure to PAs.

Author's Contributions:

Participated in research design: Guo, Zheng, Wang.

Conducted experiments: Li, Yang, Xiang, Luo, Qiu, Fang, Zhang.

Performed data analysis: Guo, Yang.

Wrote or contributed to the writing of the manuscript: Li, Yang, Guo, Zheng.

Reference

Bhattacharyya K (1965) Foetal and neonatal responses to hepatotoxic agents. *J Pathol Bacteriol* **90**: 151-161.

Chen M, Li L, Zhong D, Shen S, Zheng J, Chen X (2016) 9-Glutathionyl-6,7-dihydro-1-hydroxymethyl-5H-pyrrolizine is the major pyrrolic glutathione conjugate of retronecine-type pyrrolizidine alkaloids in liver microsomes and in rats. *Chem Res Toxicol* **29**:180-189.

Ejiri N, Katayama K, Doi K (2003) Induction of CYP3A1 by dexamethasone and pregnenolone-16alpha-carbonitrile in pregnant rat and fetal livers and placenta. *Exp Toxicol Pathol* **54**: 273-279.

Fabian E, Wang X, Engel F, Li H, Landsiedel R, van Ravenzwaay B (2016) Activities of xenobiotic metabolizing enzymes in rat placenta and liver in vitro. *Toxicol In Vitro* **33**:174-179.

Florek E, Tadrowska M, Szyfter K (1998) Tobacco smoke-induced DNA strand breaks in rat estimated by comet assay. *Toxicol Lett* **95**: 186.

Gao H, Ruan JQ, Chen J, Lin N, Ke CQ, Ye Y, Lin G, Wang JY (2015) Blood pyrrole-protein adducts as a diagnostic and prognostic index in pyrrolizidine alkaloid-hepatic sinusoidal obstruction syndrome. *Drug Des Devel Ther* **9**:4861-4868.

Gordon GJ, Coleman WB, Grisham JW (2000) Induction of cytochrome P450 enzymes in the livers of rats treated with the pyrrolizidine alkaloid retrorsine. *Exp Mol Pathol* **69**:17-26.

Gorski JC, Vannaprasaht S, Hamman MA, Ambrosius WT, Bruce MA, Haehner-Daniels B, Hall SD (2003) The effect of age, sex, and rifampin administration on intestinal and hepatic cytochrome P450 3A activity. *Clin Pharmacol Ther* **74**:275-287.

Guo Y, Ma Z, Kou H, Sun R, Yang H, Smith CV, Zheng J, Wang H (2013) Synergistic effects of pyrrolizidine alkaloids and lipopolysaccharide on preterm delivery and intrauterine fetal death in mice. *Toxicol Lett* **221**: 212-218.

Hakkola J, Pasanen M, Hukkanen J, Pelkonen O, Mäenpää J, Edwards RJ, Boobis AR, Raunio H (1996a) Expression of xenobiotic-metabolizing cytochrome P450 forms in human full-term placenta. *Biochem Pharmacol* **51**: 403-411.

Hakkola J, Raunio H, Purkunen R, Pelkonen O, Saarikoski S, Cresteil T, Pasanen M (1996b) Detection of cytochrome P450 gene expression in human placenta in first trimester of pregnancy. *Biochem Pharmacol* **52**:379-383.

Hines RN (2008) The ontogeny of drug metabolism enzymes and implications for adverse drug events. *Pharmacol Ther* **118**: 250-267.

Huybrechts B, Callebaut A (2015) Pyrrolizidine alkaloids in food and feed on the Belgian market. Food *Addit Contam Part A Chem Anal Control Expo Risk Assess* **32**: 1939-1951.

İskender-Mazman D, Akçören Z, Yiğit Ş, Kale G, Korkmaz A, Yurdakök M, Durukan T (2014) Placental findings of IUGR and non-IUGR. *Turk J Pediatr* **56**: 368-373.

Jan YH, Mishin V, Busch CM, Thomas PE (2006) Generation of specific antibodies and their use to characterize sex differences in four rat P450 3A enzymes following vehicle and pregnenolone 16alpha-carbonitrile treatment. *Arch Biochem Biophys* **446**: 101-110.

Juchau MR (1989) Bioactivation in chemical teratogenesis. *Annu Rev Pharmacol Toxicol* **29**: 165-187.

Lankas GR, Wise LD, Cartwright ME, Pippert T, Umbenhauer DR (1998) Placental P-glycoprotein deficiency enhances susceptibility to chemically induced birth defects in mice. *Reprod. Toxicol.* **12**: 457-463.

Lin G, Cui YY, Liu XQ (2003) Gender differences in microsomal metabolic activation of hepatotoxic clivorine in rat. *Chem Res Toxicol* **16**: 768-774.

Lin G, Cui YY, Liu XQ, Wang ZT (2002) Species differences in the in vitro metabolic activation of the hepatotoxic pyrrolizidine alkaloid clivorine. *Chem*

Res Toxicol **15**: 1421-1428.

Lin G, Tang J, Liu XQ, Jiang Y, Zheng J (2007) Deacetylclivorine: a gender-selective metabolite of clivorine formed in female Sprague-Dawley rat liver microsomes. *Drug Metab Dispos* **35**: 607-613.

Lin G, Wang JY, Li N, Li M, Gao H, Ji Y, Zhang F, Wang H, Zhou Y, Ye Y, Xu HX, Zheng J (2011) Hepatic sinusoidal obstruction syndrome associated with consumption of Gynura segetum. *J Hepatol* **54**: 666-673.

Longo LD, Reynolds LP (2010) Some historical aspects of understanding placental development, structure and function. *Int J Dev Biol* **54**: 237-255.

Maezawa K, Matsunaga T, Takezawa T, Kanai M, Ohira S, Ohmori S (2010) Cytochrome P450 3As gene expression and testosterone 6 beta-hydroxylase activity in human fetal membranes and placenta at full term. *Biol Pharm Bull* **33**: 249-254.

Medeiros RM, Górniak SL, Guerra JL (2000) Fetotoxicity and reproductive effects of monocrotaline in pregnant rats. *J Ethnopharmacol* **69**: 181-188.

Oropeza-Hernández LF, López-Romero R, Albores A (2003) Hepatic CYP1A, 2B, 2C, 2E and 3A regulation by methoxychlor in male and female rats. *Toxicol Lett* **144**: 93-103.

O'Shaughnessy PJ, Monteiro A, Bhattacharya S, Fowler PA (2011) Maternal

smoking and fetal sex significantly affect metabolic enzyme expression in the human fetal liver. *J Clin Endocrinol Metab* **96**: 2851-2860.

Panter KE, Gardner DR, Molyneux RJ (1998) Teratogenic and fetotoxic effects of two piperidine alkaloid-containing lupines (L. formosus and L. arbustus) in cows. *J Nat Toxins* **7**: 131-140.

Peterson JE, Jago MV (1982) Comparison of the toxic effects of dehydroheliotridine and heliotrine in pregnant rats and their embryos. *J Pathol* **131**: 339-355.

Radominska-Pandya A (2010) Preface. *Drug Metab Rev* **42**: 1-2.

Roulet M, Laurini R, Rivier L, Calame A (1988) Hepatic veno-occlusive disease in newborn infant of a woman drinking herbal tea. *J Pediatr* **112**: 433-436.

Ruan JQ, Gao H, Li N, Xue JY, Chen J, Ke CQ, Ye Y, Fu PP, Zheng J, Wang JY, Lin G (2015) Blood Pyrrole-Protein Adducts-A Biomarker of Pyrrolizidine Alkaloid-Induced Liver Injury in Humans. *J Environ Sci Health C Environ Carcinog Ecotoxicol Rev* **33**: 404-421.

Sandini TM, Udo MS, Reis-Silva TM, Bernardi MM, Spinosa Hde S (2014) Prenatal exposure to integerrimine N-oxide impaired the maternal care and the physical and behavioral development of offspring rats. *Int J Dev Neurosci* **36**: 53-63.

Sierra-Santoyo A, Hernández M, Albores A, Cebrián ME (2000) Sex-dependent regulation of hepatic cytochrome P-450 by DDT. *Toxicol Sci* **54**: 81-87.

Smith LW, Culvenor CC (1981) Plant sources of hepatotoxic pyrrolizidine alkaloids. *J Nat Prod* **44**: 129-152.

Sundareson AE (1942) An experimental study on placental permeability to cirrhogenic poisons. *J Pathol Bacteriol* **54**: 289-298.

Tu M, Li L, Lei H, Ma Z, Chen Z, Sun S, Xu S, Zhou H, Zeng S, Jiang H (2014) Involvement of organic cation transporter 1 and CYP3A4 in retrorsine-induced toxicity. *Toxicology* **322**: 34-42.

Wang YP, Fu PP, Chou MW (2005) Metabolic Activation of the Tumorigenic. Pyrrolizidine Alkaloid, Retrorsine, Leading to DNA Adduct Formation *In Vivo*. *Int J Environ Res Public Health* **2**: 74–79.

Wells PG, Bhuller Y, Chen CS, Jeng W, Kasapinovic S, Kennedy JC, Kim PM, Laposa RR, McCallum GP, Nicol CJ, Parman T, Wiley MJ, Wong AW (2005) Molecular and biochemical mechanisms in teratogenesis involving reactive oxygen species. *Toxicol Appl Pharmacol* **207**: 354-66.

Wells PG, McCallum GP, Chen CS, Henderson JT, Lee CJ, Perstin J, Preston TJ, Wiley MJ, Wong AW (2009) Oxidative stress in developmental origins of disease: teratogenesis, neurodevelopmental deficits, and cancer. *Toxicol Sci*

108: 4-18.

Wyde ME, Kirwan SE, Zhang F, Laughter A, Hoffman HB, Bartolucci-Page E, Gaido KW, Yan B, You L (2005) Di-n-butyl phthalate activates constitutive androstane receptor and pregnane X receptor and enhances the expression of steroid-metabolizing enzymes in the liver of rat fetuses. *Toxicol Sci* **86**: 281-290.

Xia Q, Zhao Y, Lin G, Beland FA, Cai L, Fu PP (2016) Pyrrolizidine Alkaloid-Protein Adducts: Potential Non-invasive Biomarkers of Pyrrolizidine Alkaloid-Induced Liver Toxicity and Exposure. *Chem Res Toxicol* **29**: 1282-1292.

Yang X, Li W, Sun Y, Guo X, Huang W, Peng Y, Zheng J (2017) Comparative Study of Hepatotoxicity of Pyrrolizidine Alkaloids Retrorsine and Monocrotaline. *Chem Res Toxicol* **30**:532-539.

Yang YC, Yan J, Doerge DR, Chan PC, Fu PP, Chou MW (2001) Metabolic Activation of the Tumorigenic Pyrrolizidine Alkaloid, Retrorsine, Leading to DNA Adduct Formation In Vivo. *Chem Res Toxicol* **14**: 101-109.

Zhou SF, Xue CC, Yu XQ, Wang G (2007) Metabolic activation of herbal and dietary constituents and its clinical and toxicological implications: an update. *Curr Drug Metab* **8**: 526-553.

Footnotes:

Xia Li and Xiaojing Yang contributed equally to this work.

Jiang Zheng

[1]Wuya College of Innovation, Shenyang Pharmaceutical University, 103 Wenhua Road, Shenyang, Liaoning, 110016, P. R. China; [2]State Key Laboratory of Functions and Applications of Medicinal Plants, Key Laboratory of Pharmaceutics of Guizhou Province, Guizhou Medical University, Guiyang, Guizhou, 550004, P. R. China.

1,2: The two corresponding units contributed equally to the work

Figure Legends

Figure 1 Pyrrole-GSH conjugates generated in microsomes treated with retrorsine (RTS). Microsomes were prepared from maternal and fetal liver as well as placenta in intact pregnant rats on gestation day 20. RTS (1 mM) was incubated with individual microsomes and NADPH in the presence of GSH. Data are shown as Mean±SEM, n=3. $^*P<0.05$, $^{**}P<0.01$ vs maternal liver, $^#P<0.05$ vs RTS treatment. According to two-way ANOVA analysis, there was no interaction between gender and RTS treatment.

Figure 2 Michaelis-Menten kinetic assessment of retrorsine (RTS) in rat maternal and fetal liver microsomes. Microsomes were incubated with RTS at various concentrations (100-8,000 μM) for 20 min. A: maternal liver microsomes; B: female fetal liver microsomes; C: male fetal liver microsomes. The unit for enzyme kinetic parameters were as follow: V_{max} (μg/min/mg protein), K_m (μM) and CL_{int} (L/min/mg protein). Data are shown as Mean±SEM, n=3.

Figure 3 Body weight of rat pups prenatally exposed to retrorsine (RTS). Pregnant rats were treated with RTS (5.0-20 mg/kg) from gestation day 9 to 20. Data are shown as Mean±SEM, n=4-11. $^{**}P<0.01$ vs control.

Figure 4 Morphologic changes of maternal and fetal liver as well as placenta. Pregnant rats were treated with RTS (5.0-20 mg/kg) from gestation day 9 to 20. The magnification for maternal and fetal liver is 200×; the magnification for placenta is 40×.

Figure 5 Concentration of serum retrorsine (RTS) in dams and fetuses. Pregnant rats

33

were treated with RTS (5.0-20 mg/kg) from gestation day 9 to 20. Horizontal bars

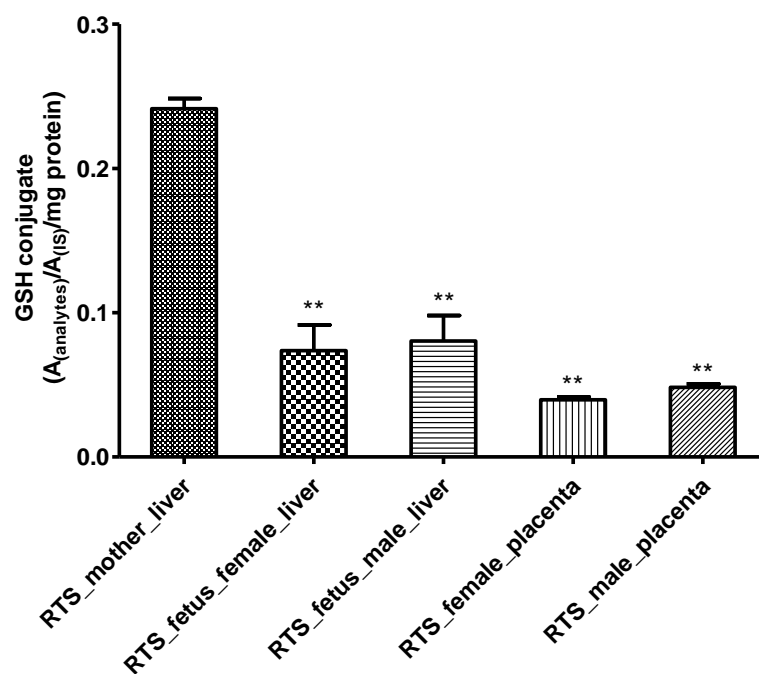represent the average serum concentration of RTS in each group, n=3-5.

Figure 6 Pyrrole-protein adduction in maternal-placental-fetal unit from pregnant rats

treated with retrorsine (RTS). Pregnant rats were treated with RTS (5.0-20 mg/kg) from

gestation day 9 to 20. Data are shown as Mean±SEM, n=3-5. $^*P<0.05$, $^{**}P<0.01$ vs

maternal liver, $^{\#\#}P<0.01$ vs female pup. According to two-way ANOVA analysis, there

was no interaction between gender and RTS treatment.

Figure 7 Effect of retrorsine (RTS) on CYP3A expression in rat fetal liver. Pregnant

rats were treated with RTS (20 mg/kg) from gestation day 9 to 20. Each well was loaded

with 50 μg of fetal liver protein or 5 μg of maternal liver microsomes as positive control.

Data are shown as Mean±SEM for gray density, n=3. $^{**}P<0.01$ vs control, $^{\#}P<0.05$,

$^{\#\#}P<0.01$ vs female pup. According to two-way ANOVA analysis, there was an

interaction between fetal gender and RTS treatment on CYP3A protein level.

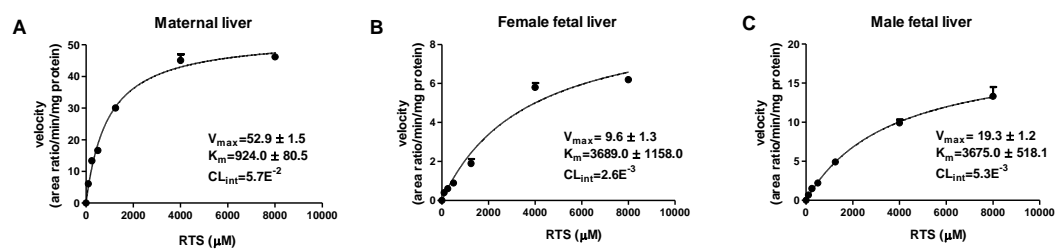Bonferroni test was used to identify significant differences among groups.

Scheme legends

Scheme 1 Proposed formation of pyrrole-GSH conjugates and pyrrole-protein adducts

as a result of RTS metabolic activation, and synthesis of compound **10** from pyrrole-

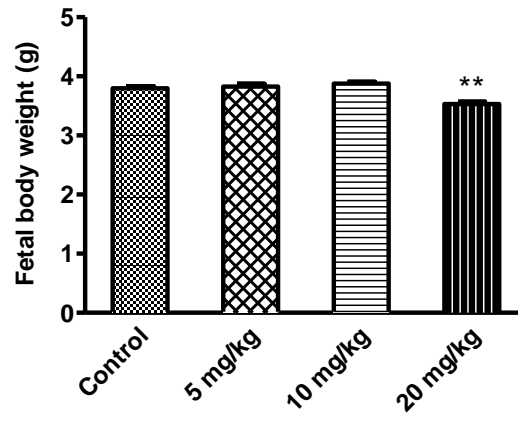protein adducts by chemical derivatization[a]. (*a*: DABA, 4-dimethylaminobenzaldehyde)
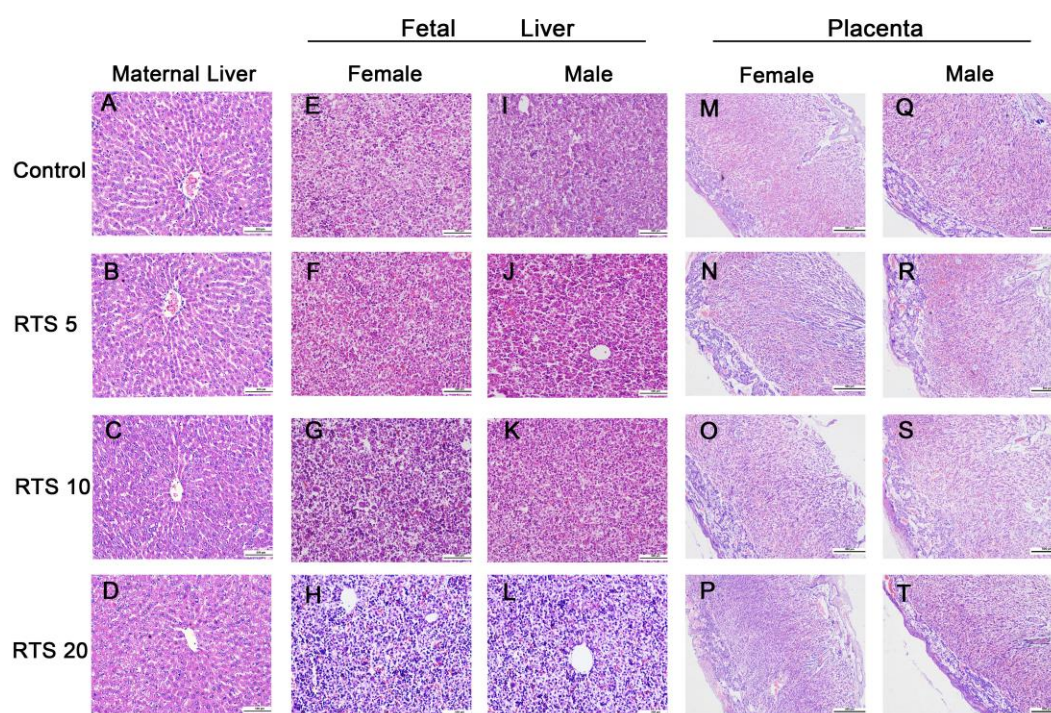
Figure 1

35

Figure 2

A Maternal liver

V_{max}=52.9 ± 1.5
K_m=924.0 ± 80.5
CL_{int}=5.7E^{-2}

B Female fetal liver

V_{max}= 9.6 ± 1.3
K_m=3689.0 ± 1158.0
CL_{int}=2.6E^{-3}

C Male fetal liver

V_{max}= 19.3 ± 1.2
K_m=3675.0 ± 518.1
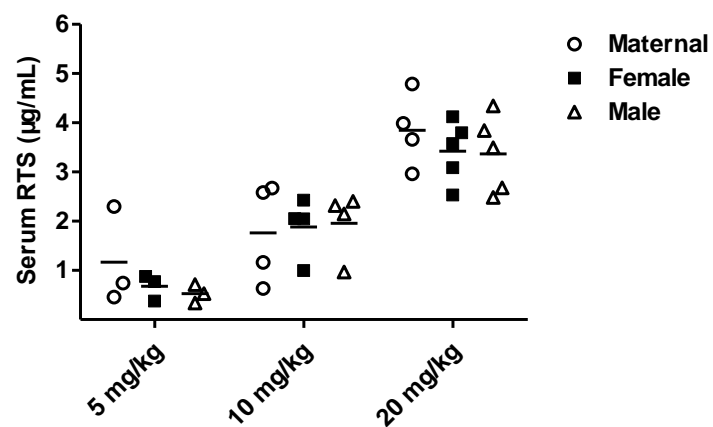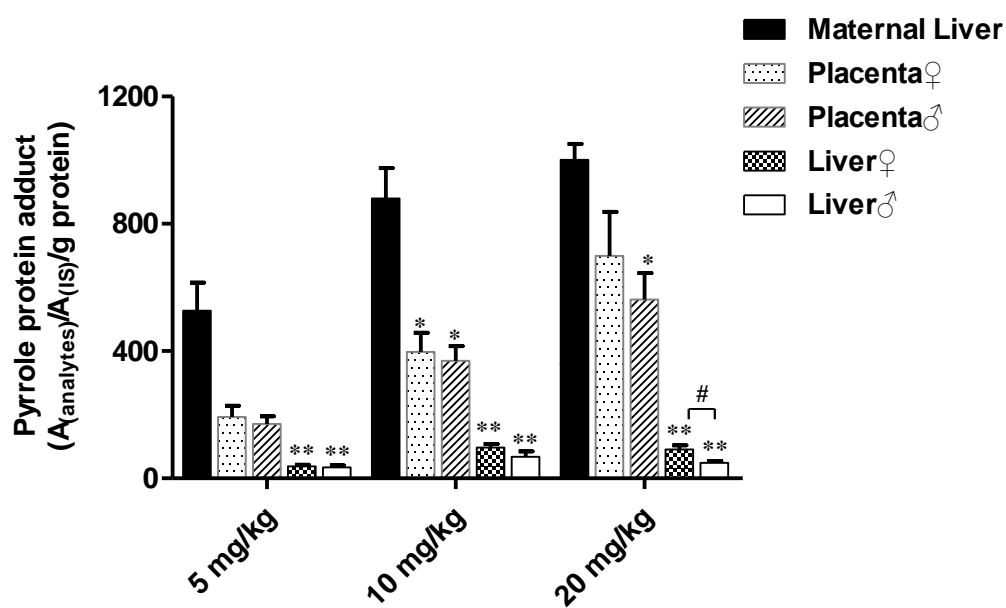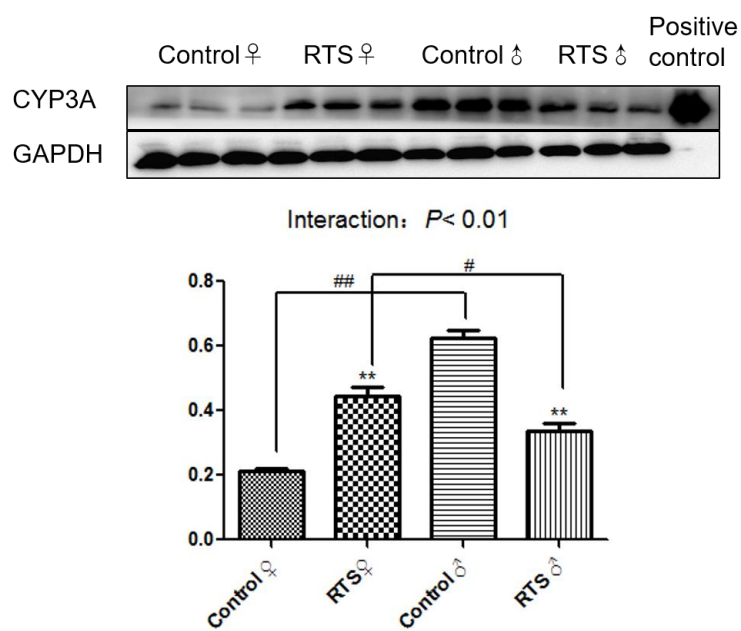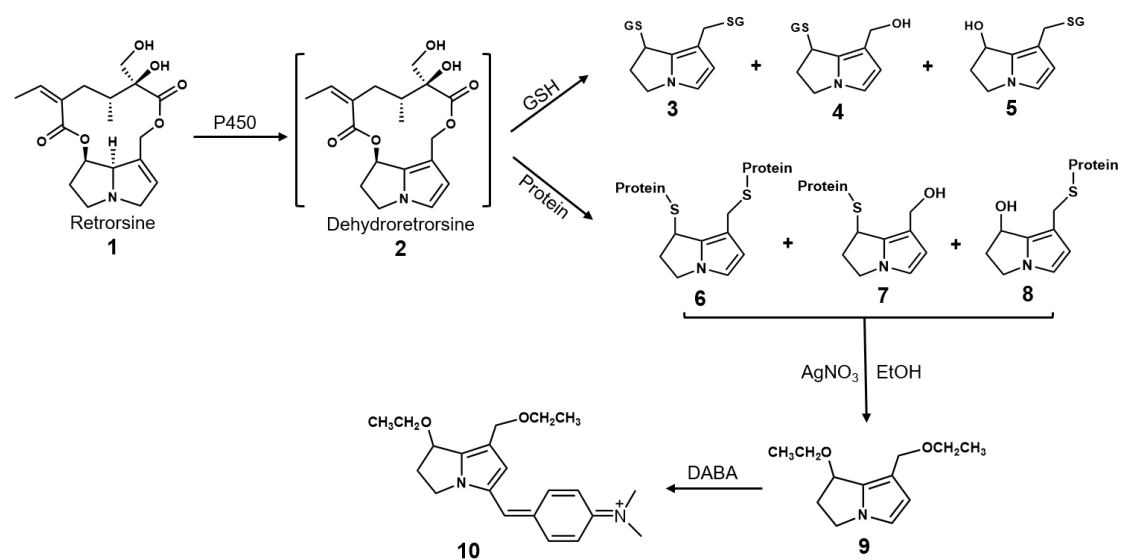CL_{int}=5.3E^{-3}

Figure 3

Figure 4

Figure 5

Figure 6

Figure 7

Scheme 1

Supplemental data for *Drug Metabolism and Disposition*

Maternal-Fetal Disposition and Metabolism of Retrorsine in Pregnant Rats

Xia Li, Xiaojing Yang, E Xiang, Jinyuan Luo, Shuaikai Qiu, Yan Fang, Li Zhang, Yu Guo, Jiang Zheng, Hui Wang

Scheme legend

Supplemental Scheme 1 Chemical synthesis of GSH conjugates **3-5** and compound **10** from monocrotaline (**11**). (DABA, 4-dimethylaminobenzaldehyde)

Supplemental Scheme 1

Monocrotaline **11** → (O-Chloranil) → Dehydromonocrotaline **12** → GSH → **3** + **4** + **5**

12 → BF$_3$·(C$_2$H$_5$)$_2$O / DABA/EtOH → **10**